ISSN: 2688-8645

# Study on Collaborative Optimization of Economic Dispatch for Demand Response of Multi-energy System in Distribution Network

Mingyang Li, Jianjun Xu, Zhifei Yang

The Electrical Information Engineering, Northeast Petroleum University, Daqing, Heilongjiang, 163318, China

## Abstract

**To address the issues of high operating costs in distribution grids and insufficient user willingness to respond to demand when a high proportion of distributed generation is connected, this study establishes a coordinated optimization model for economic dispatch and demand response that takes into account user comfort, with the aim of reducing system costs and enhancing demand-side regulation capabilities. Using a modified 33-node system as the subject, an economic dispatch model was established that includes distributed gas turbines, energy storage, photovoltaic systems, and power purchases from the main grid. The objective is to minimize total operating costs, taking into account power flow, voltage and current, and equipment constraints. The total operating cost in Scenario 2 was 16,053.38 yuan, a 4.05% reduction compared to Scenario 1; grid power purchases decreased by 6.84% (from 12,840.06 kWh to 11,962.04 kWh). Under demand response, the load adjustment rate increased, exhibiting a pattern of rising marginal costs. The ChOA algorithm converged in 13 iterations with a convergence time of 3.45 seconds, outperforming the Particle Swarm Optimization (28 iterations, 7.01 seconds) and Genetic Algorithm (24 iterations, 6.23 seconds), demonstrating stable convergence and strong robustness.**

## Keywords

**Distribution Network Economic Dispatch; User Psychological Comfort; Demand Response; Multi-energy System.**

## 1. Introduction

To address the problem of economic dispatch in distribution grids and microgrids, Reference [1] proposes a real-time economic dispatch framework based on deep reinforcement learning. It employs the DDPG algorithm to handle high-dimensional continuous action spaces, thereby enhancing online decision-making capabilities without relying on precise probabilistic models. Reference [2] addresses the issue of communication packet loss by introducing a hybrid event-triggered mechanism and switching system dynamics, enabling distributed generation units to dynamically adjust their estimates. This mitigates the adverse effects of packet loss on economic dispatch and reduces communication costs. Reference [3] addresses low-carbon building microgrids incorporating V2G by constructing a system model that includes PV, wind power, and electric vehicles. It employs an improved adaptive quantum particle swarm algorithm to solve the economic-low-carbon coordinated scheduling problem with the objective of minimizing total energy costs. Reference [4] addresses the issue of insufficient adaptability in static optimization methods for port microgrids by proposing a two-stage collaborative optimization framework that combines static demand response planning with dynamic correction based on differential evolution-reinforced learning. Reference [5] employs a load-following dispatch method to perform technical-economic modeling and capacity

ISSN: 2688-8645

optimization for hybrid PV/wind/biomass microgrids in remote areas. Reference [6] points out that the differences in fluctuations of small-capacity wind power across different time scales are often overlooked. It proposes a two-stage distributed robust economic scheduling strategy based on empirical mode decomposition, enabling equipment configuration to adapt to minute-level scheduling demands. Reference [7] investigates distributed economic scheduling for isolated microgrids under asynchronous and stochastic communication conditions, proposing a state-shift-based asynchronous consensus algorithm that achieves coordinated optimization without requiring global synchronization. Reference [8] addresses microgrids incorporating V2G by simplifying mixed-integer quadratic programming into a convex optimization problem; by combining the alternating direction method of multipliers with model predictive control, it achieves distributed solution capabilities and plug-and-play functionality in time-varying networks. Reference [9] addresses combined heat and power (CHP) microgrids by using quantile regression and rolling historical windows to estimate the joint distribution of electrical and thermal loads as well as PV generation. It constructs a probability-weighted day-ahead curve as input for deterministic mixed-integer programming, balancing uncertainty and computational efficiency. Reference [10] combines short-term economic dispatch with system adequacy assessment to quantify the economic and security value of five-minute-level dispatch, dynamic reserve requirements, battery storage, and cross-border interconnections for grids with high renewable energy penetration. Reference [11] addresses data center microgrids by integrating deterministic thermal computation with a tiered carbon trading mechanism, establishing a mixed-integer linear programming model that incorporates queueing-theory-based workload migration and waste heat recovery to achieve source-load coordinated dispatch.

In summary, current research has expanded from centralized deterministic scheduling toward data-driven, distributed, multi-timescale, and low-carbon collaborative approaches. However, there remains a need for further exploration of centralized economic scheduling models for radial distribution grids that simultaneously consider detailed power flow constraints (such as the DistFlow model) and price-incentivized demand response. Furthermore, the application of novel intelligent algorithms, such as the Chimpanzee optimization algorithm, remains insufficient. To address this, this paper establishes an economic dispatch model for distribution grids that accounts for distributed gas turbines, energy storage, photovoltaic systems, and power purchases from the main grid. It incorporates a demand response mechanism and employs the Chimpanzee Optimization Algorithm for solution.

## 2. Methods

As the proportion of various loads—such as distributed generation equipment, electric vehicles, and energy storage systems—continues to rise within distribution grids, system operation has become increasingly volatile, the difference between peak and off-peak demand has widened, and issues such as curtailed wind and solar power and grid losses have become increasingly severe. Traditional dispatch methods typically treat loads as inflexible, making it difficult to effectively utilize the resource flexibility available on the customer side. Demand response, however, leverages changes in electricity prices or incentives to encourage customers to actively adjust their electricity consumption behavior. This not only mitigates fluctuations in the load curve and alleviates supply pressure during peak hours but also helps improve the integration of renewable energy and promotes coordinated operation among generation, transmission, and consumption.

Against this backdrop, this chapter develops both an economic dispatch optimization model and a demand response model for distribution grids. The economic dispatch model aims to minimize operating costs while comprehensively considering constraints such as distributed generation, energy storage devices, and network topology. The demand response model encompasses two modes: price-driven and contract-based incentives. Building on this foundation, the chapter analyzes the coupling relationship between these two models, laying the theoretical groundwork for subsequent algorithm design and simulation validation.

## 2.1. Objective Functionn

To achieve low-carbon operation of the distribution grid, the objective is set to minimize the total system cost, and a corresponding economic dispatch model is established.

$$\begin{cases} \min B == B_{\mathrm{YX}} + B_{\mathrm{TP}} + B_{\mathrm{SOC}} + B_{\mathrm{QI}} \\ B_{\mathrm{YX}} = \sum_{t=1}^{24} C_{\mathrm{gou},t} P_{\mathrm{gou},t} \\ B_{\mathrm{TP}} = \sum_{t=1}^{24} (P_{\mathrm{G0},t} \cdot E_{\mathrm{G0},t} + \sum_{K=1}^{K} P_{\mathrm{GK},t} \cdot E_{\mathrm{GK},t}) \\ B_{\mathrm{ESS}} = \dfrac{C_{\mathrm{IN}} C_{\mathrm{RE}}}{8760} \sum_{t=1}^{24} \sum_{w=1}^{N_{\mathrm{ESS}}} P_{\mathrm{ESS},w,t} \\ B_{\mathrm{QI}} = \sum_{t=1}^{24} \sum_{q=1}^{N_{\mathrm{XNY}}} C_{\mathrm{XNY},q,t} P_{\mathrm{XNYQI},q,t} \end{cases} \tag{1}$$

where: $B$ is the total cost of the distribution system; $B_{\mathrm{YX}}$ is the operating cost of the distribution network; $B_{\mathrm{TP}}$ is the total carbon emission cost of the system; $B_{\mathrm{ESS}}$ is the operating cost of energy storage units; $B_{\mathrm{QI}}$ is the cost of curtailment of photovoltaic or wind power; $C_{\mathrm{gou},t}$ 和 $P_{\mathrm{gou},t}$ are the electricity purchase price and the purchased electricity from the main grid at time *t*, respectively; $P_{\mathrm{GK},t}$ 和 $E_{\mathrm{GK},t}$ are the active power output and the discharge carbon intensity of the distributed gas turbine at time; $P_{\mathrm{G0},t}$ 和 $E_{\mathrm{G0},t}$ are the active power purchased from the main grid and the carbon intensity of the main grid at time; $C_{\mathrm{IN}}$ 和 $C_{\mathrm{RE}}$ are the initial investment cost and the capital recovery factor, respectively; $N_{\mathrm{ESS}}$ , $N_{\mathrm{XNY}}$ are the numbers of installed energy storage units and renewable energy units, respectively; $C_{\mathrm{XNY},q,t}$ , $P_{\mathrm{XNYQI},q,t}$ are the unit penalty cost and the curtailed power of the renewable energy unit at time *t*; $P_{\mathrm{ESS},w,t}$ is the charging or discharging power of the energy storage unit at time *t*.

## 2.2. Constraints

1) Power flow constraints.

Power flow models are primarily used in radial networks and exclude the effects of voltage phase angles and current, making them suitable for finding optimal solutions in distribution network optimization and scheduling.

$$\begin{cases} P_{i,t} = \sum_{(i,j)\in\phi_1} P_{ij} - \sum_{(k,i)\in\phi_2} (P_{ki} - r_{ki} I_{ki}^2) \\ Q_{i,t} = \sum_{(i,j)\in\phi_1} Q_{ij} - \sum_{(k,i)\in\phi_2} (Q_{ki} - x_{ki} I_{ki}^2) \\ \tilde{U}_j = \tilde{U}_i - 2(r_{ij} P_{ij} + x_{ij} Q_{ij}) + (r_{ij}^2 + x_{ij}^2) I_{ij}^2 \\ I_{ij}^2 \ge \dfrac{P_{ij}^2 + Q_{ij}^2}{\tilde{U}_i} \end{cases} \tag{2}$$

where: $P_{i,t}$ , $Q_{i,t}$ are the active and reactive power at node *i* at time *t*; $P_{ij}$ , $Q_{ij}$ are the active and reactive power flowing through branch *i-j*; $\phi_1$ , $\phi_2$ is the set of all branches starting from node

$i$; $r_{ki}$, $x_{ki}$, $r_{ij}$, $x_{ij}$ is the current magnitude of branch *i-j*; $I_{ki}$, $I_{ij}$ is the current magnitude of branch *i-j*; $\tilde{U}_j$, $\tilde{U}_i$ are the squared voltage magnitudes at node *j* and node *i*.

2) Voltage and current magnitude constraints.

Since the solution to the power flow equations is not unique, additional constraints on node voltages and branch current magnitudes are imposed to ensure the thermal stability of the distribution network, thereby ensuring that the solution converges to a stable region.

$$\begin{cases} U_{i,\min}^2 \le \tilde{U}_i \le U_{i,\max}^2 \\ I_{ij}^2 \le \alpha_{ij} I_{ij,\max}^2 \\ \alpha_{ij} = \begin{cases} 1 \\ 0 \end{cases} \end{cases} \tag{3}$$

where: $U_{i,\max}$ is the maximum voltage magnitude at node *i*; $U_{i,\min}$ is the minimum voltage magnitude at node *i*; $\alpha_{ij}$ is the switching variable for the on/off state of branch *i-j*, taking a value of 1 when branch *i-j* is closed, and 0 when branch *i-j* is open.

## 2.3. Demand Response Model for Distribution Networks

The demand response process is shown in Figure 1:

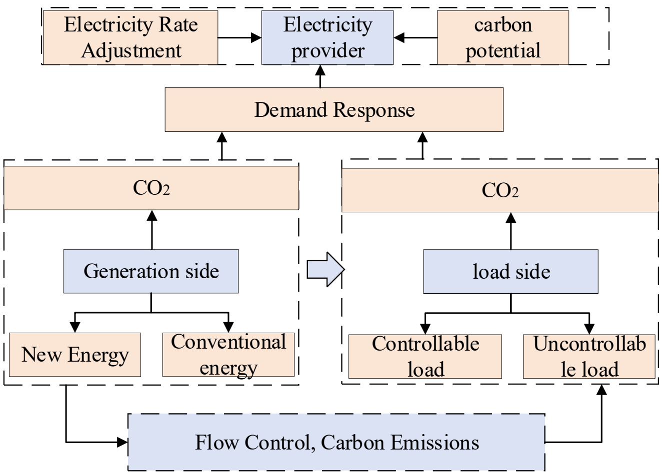


**Figure 1.** Flow chart of demand response

On the supply side, carbon emissions injected into the grid can be reduced at the source by increasing the share of clean energy and implementing carbon capture technologies. On the demand side, smart grid technologies can be leveraged to integrate demand response, flexible loads, and energy storage, enabling users to participate in system regulation and establishing a low-carbon operational system that coordinates supply and demand. Traditional dispatch focuses primarily on generation-side control, failing to fully tap into the low-carbon potential of demand-side resources. In fact, if the load side can flexibly adjust electricity consumption based on system status and market signals, it will not only improve the economic efficiency and reliability of power use but also enhance system flexibility and the capacity to integrate renewable energy. Incorporating demand-side resources into low-carbon economic dispatch is emerging as a new operational model.

This model relies on electricity price signals and dispatch instructions to dynamically regulate load, thereby enhancing regulation capacity while promoting the efficient utilization of renewable energy and driving the synergistic optimization of the power system's economic and environmental objectives. Through the organic integration of supply and demand sides, the system can further improve overall low-carbon benefits and economic efficiency while ensuring safe and stable operation.

1)Objective function.

$$f=\sum_{j=1}^{N_1}\sum_{t=1}^{24}\left(p_{\mathrm{fu},j,t}-p_{\mathrm{fd},j,t}\right)E_{\mathrm{NCEI},j,t}-\sum_{j=1}^{N_1}\sum_{t=1}^{24}p_{\mathrm{fu},j,t}P_{\mathrm{dropnew},j,t} \tag{4}$$

where: $p_{\mathrm{fu},j,t}$ , $p_{\mathrm{fd},j,t}$ are the load increase and load decrease at node *j* at time *t*; $P_{\mathrm{dropnew},j,t}$ is the amount of renewable energy curtailment at node *j* at time *t*; $M$ is the total number of nodes; $E_{\mathrm{NCEI},j,t}$ is the node carbon intensity at node *j* at time *t*.

2)Constraints

$$\begin{cases} 0\le P_{\mathrm{fu},t}\le u_{\mathrm{fu}}P_{\mathrm{fu},t}^{\max} \\ 0\le P_{\mathrm{fd},t}\le u_{\mathrm{fd}}P_{\mathrm{fd},t}^{\max} \\ \left|\sum_{j=1}^{M}P_{\mathrm{fu},j}-P_{\mathrm{fd},j}\right|=0 \end{cases} \tag{5}$$

where: $u_{\mathrm{fu}}$ , $u_{\mathrm{fd}}$ taking the value 1 for load increase and 0 for load decrease, and they cannot both be 1 at the same node; $P_{\mathrm{fu},t}$ , $P_{\mathrm{fd},t}$ are the total system load increase and load decrease at time *t*; $P_{\mathrm{fu},j}$ , $P_{\mathrm{fd},j}$ are the load increase and load decrease of the load connected to node *j* at time *t*; $P_{\mathrm{fd,t}}^{\max}$ , $P_{\mathrm{fu},t}^{\max}$ are the maximum allowable load decrease and increase of the system at time *t*.

3)Demand response costs.

When users experience a poor power supply experience due to adjustments in their power consumption, the power grid should provide them with appropriate compensation measures.

$$C_{\mathrm{DR}}=\sum_{t=1}^{24}C_1\left(P_{\mathrm{fu},t}-P_{\mathrm{fd},t}\right)\Delta t \tag{6}$$

where: $C_{\mathrm{DR}}$ is the demand response compensation cost;

## 2.4. Chimpanzee Optimization Algorithm

First, we need to randomly assign an initial position to the chimpanzee.

$$Z_{\mathrm{ch}}=\mathrm{rand}(Z_{\mathrm{sou}}-Z_{\mathrm{db}})+Z_{\mathrm{db}} \tag{7}$$

where: $Z_{\mathrm{sou}}$ is the upper bound of the search space; $Z_{\mathrm{db}}$ is the lower bound of the search space.

Then, the chimpanzees gradually closed in and surrounded their prey.

The hunting process can be described as follows:

$$\begin{cases} d_{\mathrm{A}}=\left|c_1\cdot Z_{\mathrm{A}}(n)-m_1\cdot Z_{\mathrm{ch}}(n)\right| \\ d_{\mathrm{B}}=\left|c_2\cdot Z_{\mathrm{B}}(n)-m_2\cdot Z_{\mathrm{ch}}(n)\right| \\ d_{\mathrm{C}}=\left|c_3\cdot Z_{\mathrm{C}}(n)-m_3\cdot Z_{\mathrm{ch}}(n)\right| \\ d_{\mathrm{D}}=\left|c_4\cdot Z_{\mathrm{D}}(n)-m_4\cdot Z_{\mathrm{ch}}(n)\right| \end{cases} \tag{8}$$

$$\begin{cases} Z_{\mathrm{ch}1}(n+1)=Z_{\mathrm{A}}(n)-a_1\cdot d_{\mathrm{A}} \\ Z_{\mathrm{ch}2}(n+1)=Z_{\mathrm{B}}(n)-a_2\cdot d_{\mathrm{B}} \\ Z_{\mathrm{ch}3}(n+1)=Z_{\mathrm{C}}(n)-a_3\cdot d_{\mathrm{C}} \\ Z_{\mathrm{ch}4}(n+1)=Z_{\mathrm{D}}(n)-a_4\cdot d_{\mathrm{D}} \end{cases} \tag{9}$$

$$Z(n+1)=\frac{Z_{\mathrm{ch1}}+Z_{\mathrm{ch2}}+Z_{\mathrm{ch3}}+Z_{\mathrm{ch4}}}{4} \tag{10}$$

where: $d_1$, $d_2$, $d_3$, $d_4$ are the distance between the four optimal chimpanzees and their target prey; $Z_1$, $Z_2$, $Z_3$, $Z_4$ are the relative positions of the four optimal chimpanzees with respect to their prey; $a_1$ - $a_4$, $c_1$ - $c_4$ are the elements of the corresponding coefficient vector; $m_1$ - $m_4$ are the element of the vector of chaotic mappings; $Z_{\mathrm{ch1}}$ - $Z_{\mathrm{ch4}}$ are the starting positions of the four chimpanzees;

## 2.5. Case Study Analysis

In the final stage of the hunt, the remaining chimpanzees in the four groups adjust their positions based on the optimal position of the lead chimpanzee and begin attacking the prey.

To better validate the feasibility of the model, two scenarios were established.

Scenario 1: The optimization objective is the total comprehensive cost of the distribution network, with demand response ignored. Scenario 2: This scenario corresponds to the model presented in this paper, which considers both the total operating cost of the distribution network and demand response.

This simulation analysis was conducted using the modified 33-node system for validation, as shown in Figure 2.

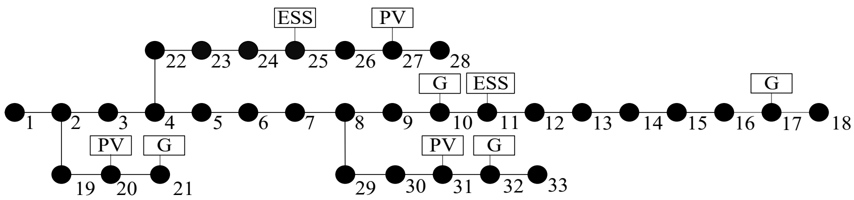


**Figure 2.** Modified 33-node system

The demand response results are shown in the figure below:

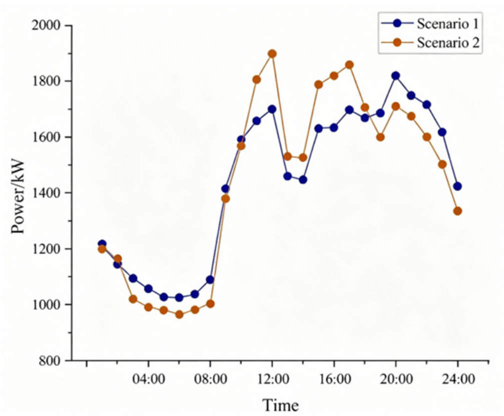


**Figure 3.** Demand response results

The load adjustment rate in Scenario 2 is higher than that in Scenario 1. As the load adjustment rate increases further, the cost of demand response shows a corresponding upward trend. This phenomenon not only aligns with the law of increasing marginal costs in demand-side resource dispatch but also reflects the characteristic that user psychological comfort gradually decreases as the magnitude of load adjustment increases. When the system further taps into peak-shaving potential, it must draw upon customer-side loads with lower response willingness or whose electricity consumption habits are more significantly affected. Consequently, higher compensation must be provided to offset the adverse effects of a diminished user experience and increased perceived costs. This phenomenon aligns with the law of increasing marginal

costs in demand-side resource dispatch: as the system taps into deeper levels of peak-shaving potential beyond existing response levels, it must progressively draw upon interruptible loads that command higher compensation prices.
The following table shows the results of the case study analysis:

**Table 1.** Results of the Case Study Analysis

| | Scenario 1 | Scenario 2 |
|---|---|---|
| Total operating cost /RMB | 16731.23 | 16053.38 |
| Electricity purchased from the grid / kWh | 12840.06 | 11962.04 |

To verify the effectiveness of the Chimpanzee Algorithm and its advantages in distribution network optimization, this paper compares the results obtained by solving Model 4 using the Chimpanzee Algorithm, the Particle Swarm Optimization (PSO) algorithm, and the Genetic Algorithm. When solving the target optimization problem using the algorithm proposed in this paper, superior solutions can be obtained. As shown in Table 3.3, the number of iterations for this algorithm is significantly lower than that of other algorithms, and it demonstrates a certain improvement in convergence speed, further validating the effectiveness of the COA algorithm.

**Table 2.** Comparison of Convergence Behavior Among Different Algorithms

| Algorithm | Number of iterations/time | Convergence time/s |
|---|---|---|
| Chimpanzee Algorithm | 13 | 3.45 |
| Particle Swarm Optimization | 28 | 7.01 |
| Genetic Algorithms | 24 | 6.23 |

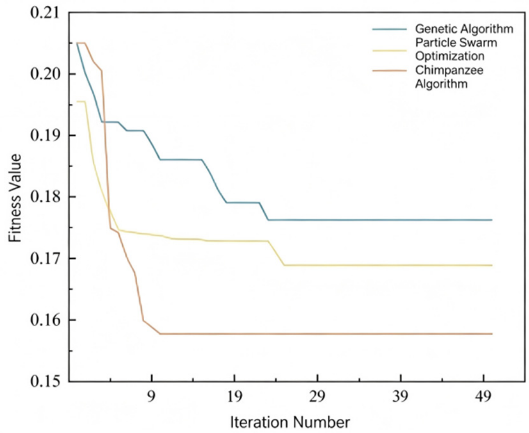


**Figure 4.** Comparative analysis of different algorithm solution processes

Combining Table and Figure reveals that when using the chimpanzee optimization algorithm for centralized solution of the model in this paper, the algorithm demonstrates significant advantages in terms of both the number of iterations and convergence time. In terms of the convergence process of fitness values, the Chimpanzee algorithm converges the fastest, rapidly approaching a stable solution, and exhibits minimal fluctuations in fitness values after convergence, demonstrating excellent stability. In contrast, although the Particle Swarm Optimization (PSO) algorithm converges more slowly, it continues to seek improvements in the later stages of iteration and ultimately obtains a superior solution; The Genetic Algorithm has an intermediate convergence speed but produces a final solution of relatively lower quality.

Overall, the Chimpanzee Algorithm not only requires fewer evolutionary generations and shorter convergence times—enabling faster optimization results—but also demonstrates superior performance in terms of optimization effectiveness and robustness. It is therefore well-suited for power distribution network optimization and scheduling scenarios where high solution efficiency is required.

## 3. Conclusion

An economic dispatch optimization model and a demand response model for distribution grids were established. With the objective of minimizing the system's total operating cost, the models account for the coordinated operation of various resources, including distributed gas turbines, energy storage systems, photovoltaic power generation, and electricity purchases from the main grid, while incorporating both price-based and incentive-based demand response mechanisms. Through simulation analysis of the improved 33-node system, two scenarios were set up: Scenario 1 without demand response and Scenario 2 with demand response. The Chimpanzee optimization algorithm was used to solve the problem. The results show that the total operating cost in Scenario 2 was 16,053.38 yuan, a reduction of approximately 4.05% compared to the 16,731.23 yuan in Scenario 1. and the electricity purchased from the main grid decreased from 12,840.06 kWh to 11,962.04 kWh, a reduction of approximately 6.84%. This indicates that demand response can effectively reduce the system's reliance on the external grid and improve economic efficiency; the demand response model achieved a higher load adjustment rate, and as the adjustment rate increased, the marginal cost followed an increasing trend, consistent with the characteristics of demand-side resource scheduling; In terms of algorithm performance, the COA algorithm demonstrated significantly fewer iterations than the Particle Swarm Optimization (PSO) and Genetic Algorithm (GA), with a stable convergence process and strong robustness, making it suitable for the rapid solution of economic dispatch problems in distribution grids. In summary, the developed model and algorithm can effectively coordinate generation, transmission, load, and storage resources to reduce overall costs while ensuring safe operation.

## References

[1] Dong, B., Cui, S., & Wang, X. (2026). A data-driven deep reinforcement learning framework for real-time economic dispatch of microgrids under renewable uncertainty. *Energies*, 19(6), 1481. https://doi.org/10.3390/en19061481.

[2] Ji, L., Du, J., Yu, F., et al. (2026). Distributed economic dispatch for smart grid subject to packet drops via hybrid event-triggered approach. *Journal of the Franklin Institute*, 363(7), 108559. https://doi.org/10.1016/j.jfranklin.2026.108559.

[3] Gong, J., Zhang, S., & Yu, F. (2026). Collaborative economic-low-carbon dispatch strategy for low-carbon building microgrid with V2G. *Journal of Physics: Conference Series*, 3198(1), 012016. https://doi.org/10.1088/1742-6596/3198/1/012016.

[4] Lu, Y., Zhu, Z., Fan, J., et al. (2026). Hybrid deep reinforcement learning for economic dispatch in port microgrids. *Applied Thermal Engineering*, 290, 130163. https://doi.org/ 10. 1016/ j. applthermaleng.2026.130163.

[5] Ezeanyanwu, N. O. U., Eke, N. M., Enibe, O. S., et al. (2026). Techno-economic modeling of hybrid PV/wind/biomass microgrid renewable energy systems using load following dispatch method. *Applied Mechanics and Materials*, 932, 103–116.

[6] Zhang, H., Dong, Y., Zhang, Y., et al. (2026). Two-stage distributed robust economic optimal dispatch of microgrid based on empirical mode decomposition (EMD). *Electrical Engineering*, 108(3), 191. https://doi.org/10.1007/s00202-025-01872-1.

[7] Sun, W., Ding, M., Huang, L., et al. (2026). Distributed economic dispatch for islanded microgrids under asynchronous and random communication conditions. *Electric Power Systems Research*, 255, 112823. https://doi.org/10.1016/j.epsr.2026.112823.

[8] Lu, F. C., Liu, P. G., Yan, R., et al. (2026). Distributed economic dispatch for microgrids with vehicle-to-grid under time-varying network. *Journal of Energy Storage*, 147, 120007. https: // doi. org/10.1016/j.est.2026.120007.

[9] Hassan, U. M. S. (2026). Dependence-aware day-ahead unit commitment and economic dispatch for a CHP-centered microgrid. *Electric Power Systems Research*, 255, 112786. https: // doi. org/10.1016/j.epsr.2026.112786.

[10] Tawoos, H. A., Cho, W. K., & Park, J. S. (2026). De-risking the transition: Quantifying the security and economic value of dynamic dispatch and integrated BESS–interconnection strategies for Egypt's high-renewable grid. *Energies*, 19(3), 786. https://doi.org/10.3390/en19030786.

[11] Ma, L., Shi, H., Liu, G., et al. (2026). Low-carbon economic dispatch of data center microgrids via heat-determined computing and tiered carbon trading. *Energies*, 19(3), 699. https:// doi. org/ 10.3390/en19030699.